Since January 2020 Elsevier has created a COVID-19 resource centre with free information in English and Mandarin on the novel coronavirus COVID-19. The COVID-19 resource centre is hosted on Elsevier Connect, the company's public news and information website.

Respiratory Medicine 170 (2020) 106036

Contents lists available at ScienceDirect

Respiratory Medicine

journal homepage: http://www.elsevier.com/locate/rmed

Chest X-ray features of SARS-CoV-2 in the emergency department: a multicenter experience from northern Italian hospitals

Davide Ippolito [a,b,*], Cesare Maino [a,b], Anna Pecorelli [a,b], Pietro Allegranza [c], Cecilia Cangiotti [c], Carlo Capodaglio [a,b], Ilaria Mariani [a,b], Teresa Giandola [a,b], Davide Gandola [a,b], Ilaria Bianco [a,b], Maria Ragusi [a,b], Cammillo Talei Franzesi [a,b], Rocco Corso [a], Sandro Sironi [b,d]

[a] Department of Diagnostic Radiology, "San Gerardo" Hospital, Via Pergolesi 33, 20900, Monza, MB, Italy
[b] School of Medicine, University of Milano-Bicocca, Via Cadore 48, 20900, Monza, MB, Italy
[c] Department of Diagnostic Radiology, Desio Hospital, Via Giuseppe Mazzini 1, 20832, Desio, MB, Italy
[d] Department of Diagnostic Radiology, H Papa Giovanni XIII, Piazza OMS 1, 24127, Bergamo, BG, Italy

ARTICLE INFO

Keywords:
Infections
Coronavirus
Radiography
Tomography
X-ray computed

ABSTRACT

Objectives: To evaluate the imaging features of routine admission chest X-ray in patients referred for novel Coronavirus 2019 infection.

Methods: All patients referred to the emergency departments, RT-PCR positive for SARS-CoV-2 infection were evaluated. Demographic and clinical data were recorded. Two radiologists (8 and 15 years of experience) reviewed all the X-ray images and evaluated the following findings: interstitial opacities, alveolar opacities (AO), AO associated with consolidation, consolidation and/or pleural effusion. We stratified patients in groups according to the time interval between symptoms onset (cut-off 5 days) and X-ray imaging and according to age (cut-off 60 years old). Computed tomography was performed in case of a discrepancy between clinical symptoms, laboratory and X-ray findings, and/or suspicion of complications.

Results: A total of 468 patients were tested positive for SARS-CoV-2. Lung lesions primarily manifested as interstitial opacities (71.7%) and AO opacities (60.5%), more frequently bilateral (64.5%) and with a peripheral predominance (62.5%). Patients admitted to the emergency radiology department after 5 days from symptoms onset, more frequently had interstitial and AO opacities, in comparison to those admitted within 5 days, and lung lesions were more frequently bilateral and peripheral. Older patients more frequently presented interstitial and AO opacities in comparison to younger ones. Sixty-eight patients underwent CT that principally showed the presence of ground-glass opacities and consolidations.

Conclusions: The most common X-ray pattern is multifocal and peripheral, associated with interstitial and alveolar opacities. Chest X-ray, compared to CT, can be considered a reliable diagnostic tool, especially in the Emergency setting.

1. Introduction

On March 11th, 2020, the World Health Organization (WHO) declared the ongoing outbreak of nCoV-2019 as a pandemic public health emergency. As of April 5th, 2020, more than 1.200.000 confirmed SARS-CoV-2 cases have been reported globally. Of these, more than 124.000 were from Italy.

The SARS-CoV-2 can manifest principally as severe pneumonia, Acute Respiratory Distress Syndrome (ARDS), and Multiple-Organ Failure (MOF), which can lead to death. The SARS-CoV-2 can be transmitted from human to human through respiratory droplets, contact, and even fecal-oral transmission [1,2].

Imaging plays an important role in the diagnosis and management of SARS-CoV-2, in particular in the case of pneumonia. Computed Tomography (CT) is considered the first-line imaging modality in highly suspected cases and helps to monitor pathological changes during treatment. Typical CT feature is the bilateral distribution of ground-glass opacities (GGOs) with or without consolidation in posterior and peripheral areas of lungs, as the cardinal hallmark of SARS-CoV-2 [3–5].

On the other hand, the routine chest X-ray is the most widely available radiological procedure during hospital admissions, in

* Corresponding author. University of Milano-Bicocca, Department of Diagnostic Radiology, H S.Gerardo Via Pergolesi 33, 20900, Monza, MB, Italy.
E-mail address: davide.atena@tiscalinet.it (D. Ippolito).

https://doi.org/10.1016/j.rmed.2020.106036
Received 22 April 2020; Received in revised form 17 May 2020; Accepted 18 May 2020
Available online 22 May 2020

Abbreviations

AO	Alveolar Opacities
ARDS	Acute Respiratory Distress Syndrome
CRP	C-Reactive Protein
CT	Computed Tomography
GGO	Ground-Glass Opacities
MERS	Middle East Respiratory Syndrome
NPV	Negative Predictive Value
PACS	Picture Archiving and Communication System
PLT	Platelets
PPV	Positive Predictive Value
RT-PCR	Reverse Transcriptase-Polymerase Chain Reaction
SARS-CoV-2	Severe Acute Respiratory Syndrome-Coronavirus-2
WBC	White Blood Cell
WHO	World Health Organization

particular, to complete differential diagnosis of respiratory symptoms, such as cough and dyspnea. The chest radiograph can establish the presence of pneumonia, define its extension and location, and can also diagnose complications. However limited information exists regarding chest X-ray imaging findings of SARS-CoV-2 lung infection [6].

Overall, due to the increasing number of reported cases of SARS-CoV-2 infection, radiologists encounter more frequently patients in the emergency setting. The goal for the radiological emergency department is to quickly undertake the diagnosis and the evaluation of patients with suspected SARS-CoV-2 and provide frontline diagnosis and confirmation of the disease. A chest X-ray may help in early detection of lung abnormalities for screening outpatients with highly suspected disease, especially in patients with an initial negative RT-PCR screening result.

The objective of our study is to describe and characterize the key findings on chest X-ray in RT-PCR SARS-CoV-2 positive patients from Lombardy, a North Region of Italy, to further help clinicians in the initial screening of patients and to familiarize the radiologists and clinical teams with the imaging manifestations of this new outbreak.

2. Materials and method

Our Institutional Review Board waived the requirement to obtain written informed consent for this retrospective case series, which evaluated de-identified data and involved no potential risk to patients, and due to the emergency condition. Moreover, no link between the patients and the researchers were made available.

2.1. Patients population

From March 1st, 2020, until March 24th, 2020, a total of 468 patients with consecutively laboratory-confirmed SARS-CoV-2 admitted at to two different emergency department (n = 283; 60.5% from Center 1, and n = 185; 39.5% from Center 2) were enrolled.

The diagnosis of SARS-CoV-2 was determined with at least two positive results of the RT-PCR assay.

For each patient, the following demographic, clinical and imaging data were recorder: 1) fever, 2) cough, 3) white blood cell count, 4) red blood cell count, 5) neutrophil count, 6) lymphocyte count, 7) platelets count, 8) C-reactive protein (CRP) leveland 9) onset of symptoms.

2.2. X-ray images

All X-ray examinations were acquired as computed or digital radiographs following usual local protocols. A standard chest X-ray was performed in anteroposterior projection only, obtained in patients at the bedside, using portable X-ray units in the isolation wards.

Images were assessed for the presence and distribution of parenchymal abnormalities including 1) alveolar opacities (AO), which were defined as a hazy increase in lung attenuation with no obscuration of the underlying vessels; 2) interstitial opacities or thickening (e.g. septal thickening or reticulation); 3) alveolar opacities associated with consolidation, which was defined as an area of opacification obscuring the underlying vessels; 4) consolidations and 5) pleural effusions.

The locations of the lesions were specified as superior, middle, and inferior, dividing the lung parenchyma into three portions. The lesions were defined as *isolated* when focal lesions involved only one portion, *multiple* when multiple areas were involved, and *unilateral* or *bilateral*.

2.3. CT images

In case of discrepancy between clinical symptoms/laboratory findings and X-ray images, and/or suspicious of complications, Computed Tomography (CT) examination was performed.

Computed tomography images were acquired using a multi-detector 256-slice scanner (iCT elite, Philips Healthcare, Eindhoven, the Netherlands) in supine patients at full inspiration and with or without contrast medium according to the clinical issue. The parameters for CT acquisition were: rotation time 0.27 ms, tube voltage 80–100 kV, automated tube-current modulation (50–70 mAs), slice thickness 0.8 mm, increment 0.4 mm, and a sharp reconstruction kernel.

To compare X-ray abnormalities with CT appearance, the following pathological features were recorded: 1) ground-glass opacities (GGOs) defined as an area of hazy increased lung opacity, 2) “reverse halo sign” defined as a focal area of ground-glass opacity surrounded by a ring of consolidation, 3) consolidation, defined as an area of homogeneous increased of pulmonary parenchyma attenuation that obscure vessels, 4) “crazy paving” pattern, defined as thickened inter and intralobular septa on a background of ground-glass opacity, 5) “tree-in-bud” pattern, that represents centrilobular branching structures often due to small airways inflammation, 6) pleural effusion.

2.4. Images analysis

Two radiologists (8 and 15 years of experience), blindly and independently, reviewed both chest X-rays and chest CT images in picture archiving and communication systems (PACS, Enterprise Imaging, AGFA Healthcare, Belgium).

2.5. Statistical analysis

Continuous variables are expressed as mean and standard deviation (SD), after assessing for normal distribution using the Kolmogorov-Smirnov test and compared using t-Student test. Categorical variables are expressed as number and percentage. A p-value < 0.05 was considered statistically significant. All the statistical analyses were performed using SPSS 21.0 statistical package (SPSS Incorporated, Chicago, Illinois, USA).

3. Results

3.1. Demographic, clinical and laboratory data of the entire cohort

A total of 468 patients were RT-PCR positive for SARS-CoV-2. The majority of patients were male (328 male, 140 female) with a mean age of 64.7 ± 14.2 years old. The majority of patients were admitted to the emergency department due to flu and respiratory symptoms (n = 458; 97.9%), while the remaining 10 were admitted for other medical illnesses (ischemic stroke and syncope). Most of them accessed the emergency department more than five days after the onset of clinical manifestations (n = 256; 57.7%). The main symptom was fever (n = 424; 90.6%), followed by cough (n = 270; 57.7%) and dyspnea (n = 266; 56.8%). Only 60 patients (12.8%) had gastrointestinal symptoms. A

small proportion of patients had just one symptom at the time of diagnosis (n = 87; 18.6%). The laboratory test revealed lymphopenia and high CRP values. The other laboratory findings along with clinical and demographic characteristic are summarized in Table 1.

3.2. X-ray features

Lung lesions primarily manifested as interstitial opacities (n = 335; 71.7%) (Fig. 1) and alveolar opacities (n = 279; 60.5%) (Fig. 2). In a non-negligible proportion of patients, a parenchymal consolidation was observed (n = 245; 52.5%), the majority of them along with alveolar opacities (n = 196; 80%) (Fig. 3). Interstitial and alveolar opacities more often involved both lungs (n = 301; 64.5%) with a peripheral predominance (n = 292; 62.5%). The medium and inferior portions of the lung were the main site of lung lesions distribution (n = 290; 62.1% and n = 335; 71.7%). In more than half of cases interstitial and alveolar opacities were located in more than one lung portion (n = 255; 54.5%) (Fig. 3). Only 57 (12.2%) patients had pleural effusion.

Patients admitted to the emergency department after 5 days from symptoms onset, more frequently had interstitial and alveolar opacities, in comparison to those admitted within 5 days (n = 199; 63% vs n = 117; 37.0%, p < 0.0001 and n = 169; 63.1% vs n = 99; 36.9%, p = 0.013), and lung lesions were more frequently bilateral, peripheral, and in more than one portion. After 5 days from symptoms onset, pleural effusion was seen more frequently (n = 45; 78,9% vs n = 12; 21,1%, p < 0.0001) (Table 2).

Older patients (>60 years) more frequently presented interstitial and alveolar opacities in comparison to younger ones (n = 215; 64.2% vs n = 120; 35.8%, p = 0.006 and n = 183; 65.6% vs n = 96; 34.4%, p = 0.005 respectively) which again were more often bilateral, peripheral located, and distributed in more than one lung portion. In older patients pleural effusion was seen more frequently (n = 44; 77,1% vs n = 13; 22,9%, p < 0.0001) (Table 2).

3.3. Comparison between X-ray and CT features

A total of 68 patients underwent a CT scan, with a mean time from X-ray of 2.3 (±2.7) days.

In 61 (89.7%) patients, chest X-rays showed abnormal features, alone or combined. CT scan confirmed the presence of lung alterations, mainly ground-glass opacities (n = 57; 93.4%) and consolidation (n = 55; 90.2%) (Fig. 4). Twenty patients had a crazy-paving pattern (32.8%) and only 2 (3.3%) and 1 (1.6%) cases a “tree-in-bud” pattern and a “reverse halo sign” pattern, respectively. The presence of pleural effusion was found in 18 (29.5%) cases (Table 3).

In those patients in whom chest X-ray was negative (n = 7; 10.3%) the CT scan revealed the presence of ground-glass opacities and consolidations (Fig. 5), alone or combined, with a bilateral and multifocal distribution in all cases. None of the patients with a negative chest X-ray had pleural effusion at CT scan.

Table 1
Clinical and demographic data of patients admitted to the Emergency Department with a positive RT-PCR test for SARS-CoV-2. Fever and cough were the most common symptoms.

	All (468)
Age (yo ± SD)	64.7 ± 14.2
Sex male (n; %)	328 (70.1)
Symptoms (n; %)	
Fever	424 (90.6)
Cough	270 (57.7)
Dyspnea	266 (56.8)
Gastrointestinal	60 (12.8)
Labs	
WBC (x 10^3/mm^3± **SD**)	7.1 ± 4.2
Neutrophils (x 10^3/mm^3± **SD**)	5.6 ± 6.0
Lymphocytes (x 10^3/mm^3± **SD**)	1.4 ± 2.8
PLT (x 10^3/mm^3± **SD**)	192.1 ± 74.6
PCR (mg/l ± **SD**)	41.4 ± 65.4

4. Discussion

Viruses are a common cause of respiratory infection and the early detection and efficient control of the route of transmission (e.g. isolation of suspected cases, disinfection) is still the most effective way to fight the SARS-CoV-2 outbreak. To date, the spread of SARS-CoV-2, according to WHO, is considered nowadays pandemic, having affected more than 100 countries all over the World [1]. In this setting, Italy is considered one of the most affected countries with more than one thousand positive cases.

According to WHO guidelines, diagnostic testing for SARS-CoV-2 is fundamental, in particular, to avoid transmission, track the epidemiology, and, finally, manage patients correctly. On the other hand, due to the large number of cases suspected for SARS-CoV-2 infection, laboratory detection is time-consuming and may not be quickly available for all people with suspected infection, with a time interval between 2 hours and 2 days. However, the main advantage of using RT-PCR assay is linked to its intrinsic high diagnostic accuracy, as previously demonstrated for influenza A, with high specificity and low sensitivity [7].

Therefore we assumed that chest X-ray can achieve the potential role of a screening test in medical settings with high disease prevalence but limited resources. In fact, in the emergency setting, the chest X-ray is a key component of the diagnostic work-up for patients with suspected infection. This paper investigates chest X-ray findings in SARS-CoV-2 patients, to increase confidence with common imaging manifestations of the disease.

We evaluated and analyzed the radiographic characteristics of 468 patients with SARS-CoV-2 pneumonia from the Emergency Radiology Unit of two tertiary and regional hospitals in Lombardy.

In our study SARS-CoV-2 primarily manifested as interstitial and alveolar opacities. Consolidations were present in 52.5%, while pleural effusion was less frequent and observed in 12.2%. The interstitial opacities and alveolar opacities may represent the radiological manifestation of pulmonary edema and hyaline membrane formation in both lungs.

Our results are not in line with the recent report of Wong et al. [8] because in our series we found a higher amount of interstitial or alveolar opacities than consolidations; these results may be due to the fact that, differently from Wong et al., we did not consider the follow-up X-ray studies that caused an increase of the number of consolidations in their series, but we focused our attention only to the typical radiographic findings encountered at emergency admittance.

In our series, lung lesions typically tend to have a peripheral distribution (62.5%), a bilateral and multifocal involvement (64.5% and 54.5% respectively), with a lower lung prevalence (71,7%), similar to SARS and MERS imaging. Moreover, we found out that consolidation is statistically associated with age >60 years old and not associated with symptoms onset (p < 0.0001 and p = 0.924 respectively), and, consistently with previous studies, SARS-CoV-2 was more often found in men than in women [9–13].

A chest radiograph can establish the presence of pneumonia, define its extension and location, and can also diagnose complications like pleural effusion, while CT can show abnormalities that are not detectable with chest radiograph, especially the less extended, due to its higher sensitivity.

In our series, only 14% of patients underwent lung CT to better evaluate parenchyma involvement, in particular those with an important discrepancy between clinical symptoms, laboratory, and chest X-ray findings.

Early radiologic investigations consistently reported that the typical SARS-CoV-2 pneumonia CT findings were bilateral ground-glass opacities (GGOs) and consolidation with a peripheral distribution, as reported by Yoon et al. [14]. In our series, CT scan confirmed the presence of different pathological findings, mainly GGO, caused by alveolar space

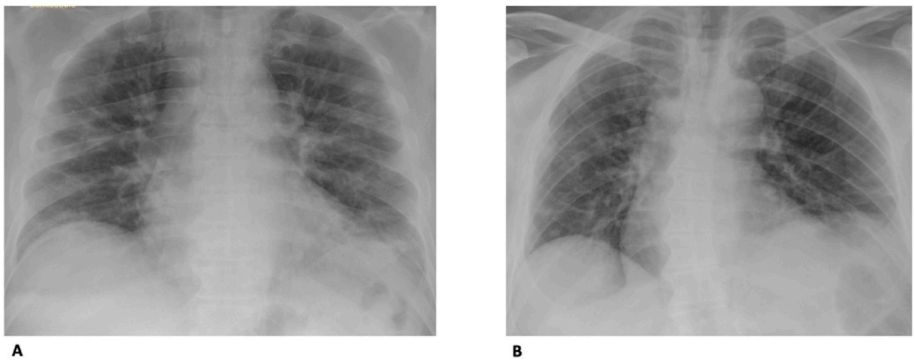

Fig. 1. Representative chest radiographic of SARS-CoV-2 pneumonia in a 56-year-old man (A) and a 61-year-old man (B) manifesting as multiple bilateral and symmetric linear interstitial opacities involving the perihilar and the peripheral zones in both of cases. No pleural effusion or consolidative lesions are evident.

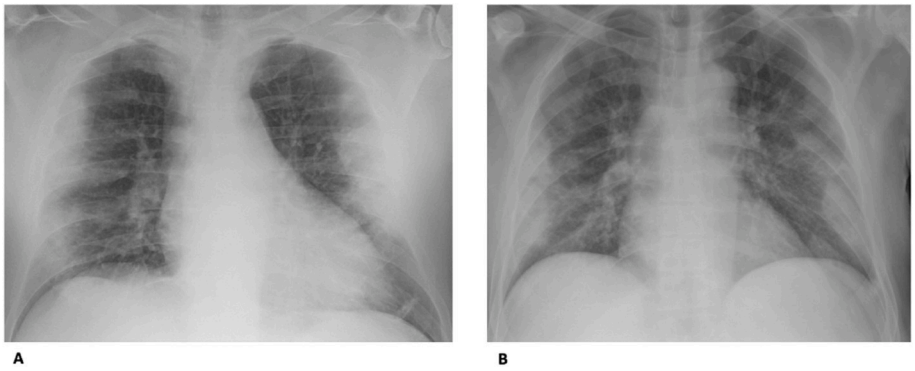

Fig. 2. Representative chest radiographic of SARS-CoV-2 pneumonia manifesting as consolidations. **A.** 71-year-old man. Anteroposterior chest radiograph shows multiple lung consolidations with typical bilateral and symmetric aspect in the middle and low part of both lungs involving the peripheral zones. **B.** 68-year-old man. Anteroposterior chest radiograph shows in the peripheral zone of both lungs multiple consolidations with the same appearance involving the middle and the inferior part of both lungs.

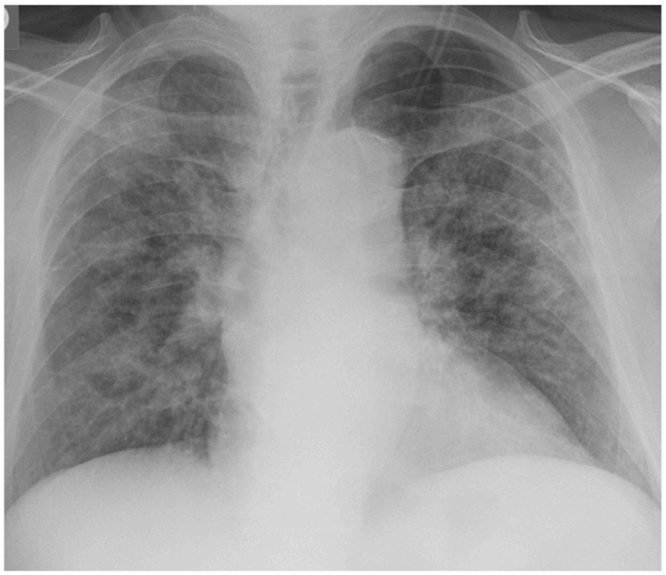

Fig. 3. Representative chest radiographic of SARS-CoV-2 pneumonia manifesting as confluent mixed alveolar and linear opacities. Anteroposterior chest radiograph shows multifocal alveolar opacities and linear interstitial opacities in both lungs.

filled with blood, pus, water, or cells, a typical finding of viral pneumonia [15]. GGO can be easily detected by using CT, primarily due to its sensitivity based on the higher spatial and contrast resolution, when compared to conventional chest X-ray. Similar results were reported from Liu et al., observing that the most common lesions were the ground glass opacities, with a typical multilobar and bilateral involvement [13].

The second most common finding in our sample was the presence of consolidation, that can also be easily demonstrated by using a chest X-ray, as we reported. These results are in line with those previously reported by using CT imaging, with a bilateral, multiple, lobular, and subsegmental areas of consolidation [13].

Moreover, our series reported a mixed pattern, composed of GGOs and consolidations, especially in patients with negative chest X-ray: this discrepancy is primarily due to the small extension of pathological findings, not detectable with the conventional radiology. Since chest X-ray is not characterized by a high spatial resolution it is not possible to evaluate the presence of crazy paving patterns, considered, moreover, a non-specific CT finding that can be seen in various conditions, especially ARDS and viral pneumonia, without a direct correspondence to plain radiograph.

On the other hand, the presence of pleural effusion can be easily detectable by using chest X-ray, even if CT permits to better evaluate its extension and, eventually, complications. Our study confirmed that none of the patients with a negative chest X-ray had pleural effusion at CT scan, encouraging the usage of chest X-ray, especially in the emergency setting and in Countries where the access to CT is lacking.

The American College of Radiology (ACR) in March 2020, discouraged CT as a screening method, firstly to reduce radiation dose exposure. However, according to the official diagnosis and treatment protocol by the National Health Commission of China [16], CT examination represents a useful tool not only in diagnosing but also in monitoring progression and therapeutic efficacy. To support this, Miao et al [17] demonstrated that the presence of diffuse ground-glass opacities could be useful in the identification and differential diagnosis of SARS-CoV-2-related pneumonia, allowing to alert clinicians for prompt treatment and repeat the RT-PCR test until the end of the incubation. Zhao et al [18], by evaluating a cohort of 101 patients, established that patients with confirmed SARS-CoV-2-related pneumonia showed typical imaging features that could be helpful in early screening of highly

Table 2
Type and distribution of lung lesions by using a cut-off of 5 days from symptoms onset and a cut-off of 60 years old. Interstitial pattern and alveolar opacities are statistically higher in patients with symptom onset >5 days and in older patients. Radiological findings are typically bilateral, subpleural and involving more than one lung portion with a statistically significant difference.

	Symptoms onest >5 days	Symptoms onest <5 days	p-value	Age >60 years (n = 281)	Age < 60 years (n = 187)	p-value
Interstitial pattern (n; %)	199 (63.0)	117 (37.0)	< **0.0001**	215 (64.2)	120 (35.8)	**0.006**
Alveolar opacities (n; %)	169 (63.1)	99 (36.9)	**0.013**	183 (65.6)	96 (34.4)	**0.005**
Consolidations (n; %)	135 (57.9)	98 (42.1)	0.924	171 (69.8)	74 (30.2)	< **0.0001**
Distribution (n; %)						
Bilateral	184 (64.6)	101 (35.4)	< **0.0001**	200 (66.4)	101 (33.6)	< **0.0001**
Subpleural	182 (65.0)	98 (35.0)	< **0.0001**	187 (64.0)	105 (36.0)	**0.032**
>1 lung portion	153 (63.7)	87 (36.3)	**0.005**	173 (67.8)	82 (32.2)	< **0.0001**
Pleural effusion (n; %)	45 (78.9)	12 (21.1)	< **0.0001**	44 (77.1)	13 (22.9)	< **0.0001**

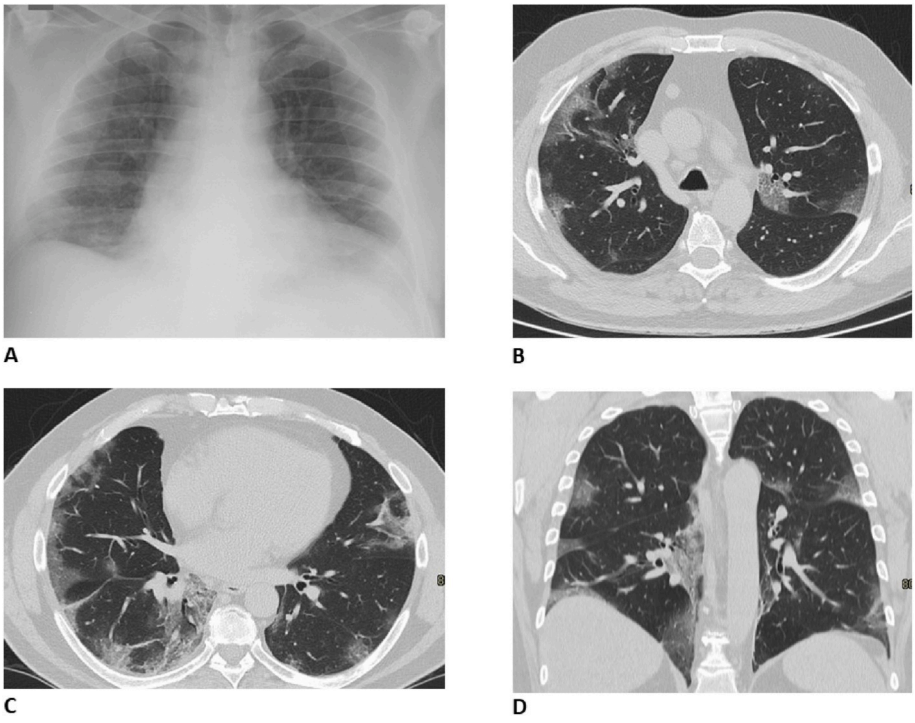

Fig. 4. Comparison between chest X-ray (A) and CT findings (B, C, D). Chest X-ray shows slightly linear opacities in the lower portion of the right lung. CT axial images (B and C in the axial plane, D in the coronal plane) with window width and level for the evaluation of lung parenchyma allow us to correctly found out the presence of multiple bilateral ground-glass opacities, especially in the subpleural space.

Table 3
Type of lung alternations in those patients who underwent a CT scan because of a discrepancy between clinical symptoms/laboratory findings and x-ray images, and/or suspicious of complications. The most frequent abnormalities at chest CT in a patient with known Sars-Cov-2 infections are ground-glass opacities and consolidations.

	All (n = 68)	Patients with negative X ray (n = 7)
Ground glass opacities (n; %)	57 (93.4)	5 (7.1)
Consolidations (n; %)	55 (90.2)	5 (7.1)
Crazy paving pattern (n; %)	20 (32.8)	–
Tree in bud (n; %)	2 (3.3)	–
Reverse halo sign (n;%)	1 (1.6)	–
Pleural effusion (n; %)	18 (29.5)	–

suspected cases. Moreover, according to Fang et al [19], the sensitivity of chest CT was statistically greater than RT-PCR (98% vs 71%), encouraging the use of CT as a screening test in patients with clinical and epidemiological features compatible with SARS-CoV-2 infection. The RT-PCR test can show a low efficiency probably due to the low viremia and the unsuitable clinical sampling. On these bases, as suggested by our results, CT plays an important role both in diagnosis, especially the differential, and in clinically suspected patients with negative chest radiograph due to its intrinsic higher sensitivity. Finally, even if different studies evaluated the role of CT as a routine imaging modality for diagnosis or screening, the use of CT is rather complex, especially in the Emergency Department, first of all, due to time-consuming decontamination procedures to be completed in the CT room among different patients [10].

Our study had some limitations. First of all, most of our patients did not undergo a CT scan examination, therefore some early radiological lung features may not be demonstrated. Second, we did not evaluate follow-up X-ray findings in our study. Finally, some of the radiographic features were subtle, thus may limiting the reproducibility in suboptimal viewing conditions or by non-specialists.

5. Conclusion

In conclusion, although usually viral pneumonia has no typical

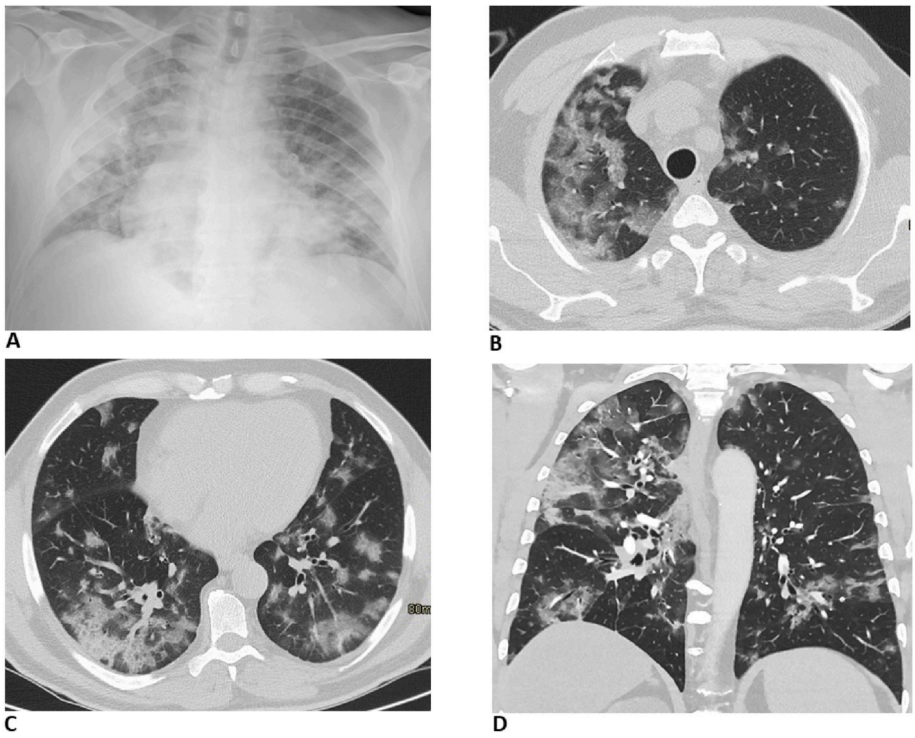

Fig. 5. Comparison between chest X-ray (A) and CT findings (B, C, D). Chest X-ray shows the presence of multiple confluent mixed alveolar and linear opacities, distributed bilaterally. CT axial images (B and C in the axial plane, D in the coronal plane) with window width and level for the evaluation of lung parenchyma allow to correctly found out the presence of multiple and confluent GGOs, distributed in particular in the right lung, especially in the subpleural area.

imaging patterns, most of the cases with SARS-Cov-2 infection have similar manifestations on imaging and are related to the pathogenesis of pulmonary viral infection.

The most common X-ray pattern findings are interstitial and alveolar opacities, with a multifocal and peripheral pattern, with distribution slightly predominant in the lower lung.

These results demonstrated that the most common CT findings can be also appreciated on X-ray, that should be considered as a useful diagnostic imaging tool especially in the emergency setting or in those hospitals and country where the CT is not always available.

Declaration of competing interest

The authors declare that they have no known competing financial interests or personal relationships that could have appeared to influence the work reported in this paper.

CRediT authorship contribution statement

Davide Ippolito: Project administration, Supervision, Writing - review & editing, Writing - original draft, Data curation, Conceptualization. **Cesare Maino:** Project administration, Writing - original draft, Writing - review & editing. **Anna Pecorelli:** Project administration, Writing - review & editing, Writing - original draft, Formal analysis. **Pietro Allegranza:** Investigation. **Cecilia Cangiotti:** Data curation. **Carlo Capodaglio:** Data curation, Resources, Investigation. **Ilaria Mariani:** Data curation, Resources, Investigation, Software. **Teresa Giandola:** Data curation, Investigation. **Davide Gandola:** Investigation. **Ilaria Bianco:** Investigation. **Maria Ragusi:** Data curation. **Cammillo Talei Franzesi:** Project administration, Methodology. **Rocco Corso:** Validation. **Sandro Sironi:** Visualization, Supervision.

Acknowledgments

We would like to thank all the radiographers that have dedicated their time and efforts to perform the several radiological SARS-CoV-2 examinations in the isolation wards during this time and the radiologist staff of both hospitals to support that work.

References

[1] E. Callaway, Time to use the p-word? Coronavirus enters dangerous new phase, Nature d41586-020-00551–1, https://doi.org/10.1038/d41586-020-00551-1, 2020.
[2] J. Gu, B. Han, J. Wang, COVID-19: gastrointestinal manifestations and potential fecal-oral transmission, Gastroenterology (2020), https://doi.org/10.1053/j.gastro.2020.02.054.
[3] J.Y.-H. Hui, T.Y.-W. Hon, M.K.-W. Yang, et al., High-resolution computed tomography is useful for early diagnosis of severe acute respiratory syndrome–associated coronavirus pneumonia in patients with normal chest radiographs, J. Comput. Assist. Tomogr. 28 (2004) 1–9, https://doi.org/10.1097/00004728-200401000-00001.
[4] J. Wei, H. Xu, J. Xiong, et al., 2019 novel coronavirus (COVID-19) pneumonia: serial computed tomography findings, Korean J. Radiol. 21 (2020) 501, https://doi.org/10.3348/kjr.2020.0112.
[5] Y.-H. Xu, J.-H. Dong, W.-M. An, et al., Clinical and computed tomographic imaging features of novel coronavirus pneumonia caused by SARS-CoV-2, J. Infect. 80 (2020) 394–400, https://doi.org/10.1016/j.jinf.2020.02.017.
[6] N. Chen, M. Zhou, X. Dong, et al., Epidemiological and clinical characteristics of 99 cases of 2019 novel coronavirus pneumonia in Wuhan, China: a descriptive study, Lancet 395 (2020) 507–513, https://doi.org/10.1016/S0140-6736(20)30211-7.
[7] B. Stone, J. Burrows, S. Schepetiuk, et al., Rapid detection and simultaneous subtype differentiation of influenza A viruses by real time PCR, J. Virol Methods 117 (2004) 103–112, https://doi.org/10.1016/j.jviromet.2003.12.005.
[8] H.Y.F. Wong, H.Y.S. Lam, A.H.-T. Fong, et al., Frequency and distribution of chest radiographic findings in COVID-19 positive patients, Radiology (2019), https://doi.org/10.1148/radiol.2020201160, 201160.
[9] H.X. Bai, B. Hsieh, Z. Xiong, et al., Performance of radiologists in differentiating COVID-19 from viral pneumonia on chest CT, Radiology (2020), https://doi.org/10.1148/radiol.2020200823, 200823.
[10] F. Pan, T. Ye, P. Sun, et al., Time course of lung changes on chest CT during recovery from 2019 novel coronavirus (COVID-19) pneumonia, Radiology (2020), https://doi.org/10.1148/radiol.2020200370, 200370.
[11] S.H. Yoon, K.H. Lee, J.Y. Kim, et al., Chest radiographic and CT findings of the 2019 novel coronavirus disease (COVID-19): analysis of nine patients treated in korea, Korean J. Radiol. 21 (2020) 494–500, https://doi.org/10.3348/kjr.2020.0132.

[12] Z. Xu, L. Shi, Y. Wang, et al., Pathological findings of COVID-19 associated with acute respiratory distress syndrome, Lancet Respir. Med. 8 (2020) 420–422, https://doi.org/10.1016/S2213-2600(20)30076-X.
[13] T. Liu, P. Huang, H. Liu, et al., Spectrum of chest CT findings in a familial cluster of COVID-19 infection, Radiology: Cardiothorac. Imag. 2 (2020), e200025, https://doi.org/10.1148/ryct.2020200025.
[14] Soon Ho Yoon, Kyung Lee, Jin Kim, Young Lee, Hongseok Ko, Ki Kim, Chang Min Park, Yun-Hyeon Kim, Chest radiographic and CT findings of the 2019 novel coronavirus disease (COVID-19): analysis of nine patients treated in korea, Korean J. Radiol. 21 (2020), https://doi.org/10.3348/kjr.2020.0132.
[15] Tomás Franquet, «Imaging of pulmonary viral pneumonia», Radiology 260 (1) (2011) 18–39, https://doi.org/10.1148/radiol.11092149, luglio, DOI.org (Crossref).
[16] National Health Commission of the People's Republic of China, The diagnostic and treatment protocol of COVID-19. China, Available via, http://www.gov.cn/zhengce/zhengceku/2020-02/19/content_5480948.htm, 2020. Accessed 3 Mar 2020.
[17] C. Miao, M. Jin, L. Miao, et al., Early chest computed tomography to diagnose COVID-19 from suspected patients: a multicenter retrospective study, Am. J. Emergency Med. (2020), https://doi.org/10.1016/j.ajem.2020.04.051. S0735675720302813.
[18] W. Zhao, Z. Zhong, X. Xie, et al., Relation between chest CT findings and clinical conditions of coronavirus disease (COVID-19) pneumonia: a multicenter study, Am. J. Roentgenol. 214 (2020) 1072–1077, https://doi.org/10.2214/AJR.20.22976.
[19] Y. Fang, H. Zhang, J. Xie, et al., Sensitivity of chest CT for COVID-19: comparison to RT-PCR, Radiology (2020), https://doi.org/10.1148/radiol.2020200432, 200432.